Fermilab Library
0 1160 0033699 4

CWRU-P4-94
March 1994

THE SUN AS A PROBE OF VARYING G

P. Demarque[1], Lawrence M. Krauss[2], D. B. Guenther[1,3], and David Nydam[1]

[1]Center for Solar and Space Research, Department of Astronomy, Yale University,
P.O. Box 6666, New Haven, CT 06511
[2]Departments of Physics and Astronomy, Case Western Reserve University,
10900 Euclid Ave, Cleveland OH 44106-7079
[3]Department of Astronomy and Physics, Saint Mary's University, Halifax, N.S.,
CANADA, B3H 3C3 St. Mary's U., Halifax

NAME	I.D. NO.	M.S.

RETURN TO FERMILAB LIBRARY

ABSTRACT

In order to explore the ability of helioseismology, and features of solar models to test the constancy of the gravitational constant G during the last 4.5 Gyr of solar evolution, we have constructed a grid of evolutionary sequences for solar models under the assumptions that G varies with time, and explored the sensitivity of their non-radial acoustic mode oscillation spectrum to G variability. All final models satisfy the standard constraints for the present Sun and except for the variation in G, were constructed under the assumptions of a standard solar model. When compared to the observed solar p-mode spectrum, our models definitely rule out $\beta > 0.4$ and $\beta < -0.4$, where $G(t) \propto t^{-\beta}$ over the last 4.5 Gyr. These limits can be tightened to rule out $|\beta| > O(0.1)$ by the use of other solar observables. For non-monotonic variation in G this suggests long timescale variations greater than O(5%) in G are ruled out over the last 4.5 Gyr. Future prospects for improving the sensitivity of helioseismic tests of a varying G are also discussed. Finally, we explore the sensitivity of the predicted solar neutrino flux to varying G.

1. INTRODUCTION

The possibility that the universal gravitational constant G varies with time was first introduced by Dirac (1938) on the basis of his large number hypothesis in an attempt to provide a "new basis for cosmology." Since Dirac, various astronomical and cosmological implications of a variable G have been discussed by a number of authors (see, e.g., the early review by Wesson 1973). The theory of gravitation of Brans and Dicke (1961) has attracted particular attention because it was designed to modify general relativity by incorporating Mach's principle, which is incompatible with general relativity. One of the perceived cosmological advantages of the Brans-Dicke idea was a reduction of the ages of the globular clusters, the oldest dated objects, to values more compatible with the universal expansion time scale (Dicke and Peebles 1965).

In the past several years there has been a resurgence of interest in the possibility of varying G cosmology. Motivated first by re-examination of Kaluza-Klein ideas for unification of gravitation with other gauge theories (e.g., Marciano 1984) and leading eventually to more workable superstring theories, the notion that G is a dynamical quantity appears quite natural. In essentially all of these theories, a dilaton scalar field is coupled to the scalar curvature R in such a way that the strength of gravity is related to the expectation value of this scalar field, in a Brans-Dicke (BD) like manner. Unlike the simple BD theory however, the couplings of this field can be of arbitrarily high order (i.e., see Steinhardt and Accetta 1990). In addition, one can arrange a scalar field potential which can lead to interesting dynamical behavior as a function of cosmic time.

Perhaps the most interesting use of these ideas for cosmology has involved an attempt to resuscitate so-called "old" inflation, involving a first order transition at some Grand Unified Scale. Traditionally, "old" inflationary models suffered from the fact that exponential expansion during the phase transition implied that the transition could not complete in a satisfactory manner. However, it was argued (La and Steinhardt 1989) that

a varying G during the transition could effectively change an exponential expansion to a power-law expansion. In this case the transition could gracefully complete itself.

One of the major challenges to such a scenario are the very tight limits set on the variation of the gravitational constant at the present time, primarily from radar measurements of planetary motions (Shapiro 1964; Shapiro et al. 1971;Reasenberg 1983) and pulsar timing measurements (Damour et al. 1988). These all suggest that $\dot{G}/GH < 0.4$ today, where H is Hubble's constant. It was soon recognized, however, that it might be possible to design the dynamical evolution of G so that at late times this variation would disappear, and the theory would approach GR (e.g., Steinhardt and Accetta 1990).

Very strong limits have been placed on the magnitude of G during Big Bang Nucleosynthesis in order to maintain consistency with observations (e.g., Accetta, Krauss and Romanelli 1990). When expressed as a limit on a monotonic variation of G of the form $t^{-\beta}$, one finds a limit $\beta < 0.008$. However, such an extrapolation, involving a monotonic variation back until times of order seconds, may not be appropriate. It is thus worth probing the magnitude of G during intermediate times, between the Big Bang and today. (i.e. see, Krauss and White 1992).

These developments not only motivate a new interest in the possibility of varying G cosmology, but they also underscore the importance of supplementing existing limits on variations at the present time by probes which can constrain the variation of G over cosmic time. Here, we re-examine the limits which can be placed on variations in G by existing probes of the Sun. Not only does the solar age provide a nice intermediate cosmic time scale to examine such variations, but it is well known that stellar evolution will depend sensitively on the magnitude of G. In addition, arbitrary (small) variations of G can be consistently incorporated into stellar evolution codes (as long as the corrections to GR remain small), without regard to the ability, or lack thereof, to derive detailed analytical cosmological models which accommodate such variations (as is necessary in other tests). Indeed, only for the simple Brans-Dicke model has a detailed cosmology

been worked out. We will present here limits on variations of G that focus on an approximate power-law monotonic variation over the Solar lifetime. For small variations, or long time oscillations, this should provide a good idea on the overall magnitude of the constraints solar structure and evolution models provide.

Solar evolution with varying G has been studied by Pochoda and Schwarzschild (1964), Ezer and Cameron (1966), Roeder and Demarque (1966) and Shaviv and Bahcall (1969). The effects of varying G on stellar evolution near the main sequence turnoff have been investigated by Roeder (1967), Gamow (1967) and Prather (1976). Giant stars have been considered by Tinsley (1972) and Prather (1976).

Helioseismology offers a independent way of probing the value of G during the last 4.5 Gyr, the evolutionary lifetime of the Sun. Because the luminosity of the Sun depends sensitively on G (Teller 1948), the amount of hydrogen converted into helium (or more conveniently, the helium abundance profile) is a function of the history of the value of G during solar evolution. In a standard model of the present Sun, this is reflected in the depth of the convection zone (the mixing length parameter α), the surface helium abundance, and the mass stratification of the models (Demarque and Guenther 1991). All these factors in turn determine the details of the run of the sound speed throughout the solar interior and the frequencies of the acoustic non-radial oscillation spectrum (p-mode spectrum). The frequencies are directly determined from either Doppler shift measurements of the Sun's surface or luminosity variations. The degree of a mode can be inferred from its horizontal wavenumber which is given by:

$$k_h^2 = l(l+1)/R_s^2.$$

When a p-mode propagates downward the wave front is "refracted" back towards the surface by the ever increasing sound speed with depth. The inner turning radius of the p-modes, i.e., the maximum depth a mode feels, depends on the frequency and degree of the mode. Figure 1 shows the inner turning radius for modes of different degrees and

cyclic frequencies ω. Because different modes penetrate to different depths they, i.e., their frequencies, are sensitive to the interior structure to differing degrees. One can, for example, calculate p-mode frequencies of a model of the Sun and then infer from comparisons of the model's spectrum and the Sun's oscillation spectrum where the structure of the model and the structure of the Sun differ. In fact this form of analysis, i.e., solar seismology, has been utilized to fine tune the solar model.

Currently, the oscillation spectra of the most sophisticated solar models differ from the Sun's oscillation spectrum by approximately ±0.2%. The existing discrepancy is believed to be primarily due to errors in the opacities and equation of state used in the model. The oscillation frequencies can be observed to an accuracy that exceeds ±0.01% for some modes and is typically ±0.05% for modes with degree less than 100 in the 2000 to 4000μHz range (the acoustic cut-off frequency of the solar model is near 5000μHz).

Another type of oscillation is predicted to exist, the *g*ravity mode (g-mode) oscillation; so named because the restoring force is due to buoyancy or gravity. The g-mode spectrum also depends on the local physical conditions in the solar interior, and in particular, the deep interior, but the definitive identification of g-modes at the Sun's surface has not yet been made. As a result, while such oscillations provide a more direct, and more stringent limit, we focus here on p-modes, for which theory can confront observation. (In Guenther at al. 1994 the potential for g-modes to provide stronger constraints will be discussed). We also explore other "observables" associated with solar evolution which can be used to constrain variations in G.

In the following section we briefly describe the assumptions used to construct and pulse solar models in a varying G universe. In § 3 we describe the results of our calculations and, in particular, compare the oscillation spectra of the models to the oscillation spectrum of the Sun. In § 4 we describe the significance of the main results of our work.

2. METHOD

The process of constructing a solar model is well defined (e.g., Demarque and Guenther 1991). Basically it involves numerically calculating the run of density, temperature, luminosity, and composition, as a function of radius and time for a one solar mass star, that, after 4.5 Gyr of evolution, has the observed radius and luminosity of the Sun. A zero age main sequence model of the Sun, i.e., a homogenous spherical distribution of the basic elemental constituents of the Sun in hydrostatic equilibrium, is input into the stellar evolution code and allowed to evolve. Evolution occurs as the central nuclear reactions convert four hydrogen atoms (protons) into one helium atom (^{4}He) and as the regions surrounding the core fall toward the center to maintain hydrostatic equilibrium (see, e.g., Schwarzschild 1958). After 4.5 Gyr of evolution, the age of the Sun (Guenther 1989), a model of the Sun is produced. Without fine tuning, the model will have neither the observed radius nor the observed luminosity. The radius of the model of the Sun is largely determined by the mixing length theory which is used to model the turbulent convection that takes place in the outer envelope of the Sun. Convection is responsible for transporting energy and mixing the chemical constituents. The luminosity of the model of the Sun is largely determined by the fraction of helium in the model. Increasing the fraction of helium in the model increases the average molecular weight per unit volume of star material, μ, which, in turn, increases the nuclear luminosity ($L \propto \mu^{7.5}$). The mixing length theory, as implemented in most stellar evolution calculations, contains a free parameter, the mixing length parameter, α, that characterizes how many pressure scale heights a convective element rises before it equilibrates (i.e., dissolves) into its surroundings. This number is unknown and is adjusted so that the model has the correct radius. Because the surface of the Sun is only 5780K, it is not hot enough to show helium lines in its spectrum; hence, the abundance of helium is

considered a free parameter of the model. It is adjusted so that the model has the correct luminosity.

As outlined earlier, to model the evolution of the Sun for varying G we replaced the constant G with a power law function:

$$G(t) = G_0\left(\frac{t_0}{t}\right)^{\beta}$$

where, t_0 is the present day age of the Universe, G_0 is the present day value of the Gravitational Constant, and β is an arbitrary power. For the calculations presented here we have taken $G_0 = 6.67259\times10^{-8}$ cm^3 g^{-1} s^{-2} (Cohen and Taylor 1986) and the age of the Universe as 15 Gyr. The precise values of these numbers are not critical to the conclusions drawn from this work.

Because varying G does affect the structure of the model, it is necessary to re-tune each model to the solar radius and luminosity, by adjusting the mixing length parameter and helium abundance. Models were calculated for powers varying from β=–0.400 to β=0.400.

The tuned models were input in Guenther's nonradial, nonadiabatic stellar pulsation code and the frequencies of a broadly selected sample of p-modes were calculated. The stellar pulsation code solves the linearized nonadiabatic nonradial oscillation equations (Saio & Cox 1980; Guenther 1993) using the Henyey relaxation method. The models and some of their properties are summarized in Table 1. The models and their oscillation spectra are discussed in the next section.

3. RESULTS

3.1 Structure of the Solar Model

In this section we address following questions: (1) how does a varying G cosmology affect the structure of the solar model? (2) how does a varying G cosmology affect the p-mode frequencies? (3) is the perturbation to the frequencies observable? (4) what is the upper limit variation that can be detected using the Sun's p-mode frequencies, (5) does stellar theory offer any other observables that can be used to study varying G cosmology?

As can be seen in figure 2, with $\beta = 0.100$ the value of G changes by less than 4% over the 4.5 Gyr lifetime of the Sun. Remarkably, this small variation in G does alter the structure of the Sun enough to result in significant perturbations to the frequencies of the p-modes. Figure 3a and 3b show the evolution of the solar models in the HR-diagram. These evolutionary tracks can be used to rule out the more extreme values for the variations in G. For $\beta < -0.100$ and for $\beta > 0.100$ the tracks are significantly distorted compared to the standard track for the Sun. These extreme departures from standard evolution carry the sun to regions where, for example, the earth could not sustain life, or all water would be in vapor form.

The effect of a slowly varying G on the evolution of a star is felt primarily through the Poisson equation describing the gravitational potential Φ:

$$\nabla^2\Phi = G4\pi\rho r^2$$

Increasing or decreasing G is effectively the same as increasing or decreasing the mass or average density of the star. Increasing the mass of a star, or equivalently its average density, increases its average mean molecular weight μ, which, as stated above, strongly affects the luminosity of the star. For homologous models, it can be shown that the luminosity of a star is also proportional to $G^{7.5}$ (Teller 1948, Schwarzschild 1958).

During the normal evolution of the Sun from zero age to its current age, the conversion of hydrogen into helium slowly increases the mean molecular weight in the interior. Both the luminosity and radius of the Sun increase as the Sun evolves, i.e., the Sun moves upwards and to the left in the HR-diagram. Since small variations in G can lead to large variations in the luminosity of the star it is not too surprising that the evolutionary tracks of the Sun are affected by the varying G models. For evolutionary tracks of the Sun with $\beta > 0.0$, the Sun starts off with G greater than the current value (G_0), hence, it looks like a zero age main sequence star of higher mass. The higher value of G places the zero age Sun at a higher than normal luminosity because on the zero age main sequence the luminosity and surface temperature of a star increases with increasing mass. As the solar model evolves and the value of G decreases, the model follows a path that leads it to the Sun's observed position in the HR-diagram. Although the varying G solar models end up in the same position in the HR-diagram as the constant G solar model, their interior structure is not the same. This is because the average luminosity of the varying G models are higher, and as a result they burn more hydrogen during their 4.5 Gyr lifetime, hence, are effectively "older" than the constant G solar model. In fact, this is why one predicts younger ages for globular clusters in a Brans-Dicke cosmology: the star burns its fuel more quickly, and hence passes through the various phases of evolution sooner (Dicke and Peebles 1965; Roeder 1967; Prather 1976).

We also note that for $\beta < -0.100$, the Sun is less luminous at any given age compared to the evolution of a standard solar model. This would, we speculate, strongly affect the development of life on earth. For example, if $\beta = -0.200$, then when the Sun is 3 Gyr old it would be 40% fainter than the standard solar model at that time. It seems unlikely that with such a large departure from the standard predicted luminosity of the Sun could be tolerated with respect to the development of life. A careful analysis is required to quantify this statement. Similarly, the ages of the globular clusters would be

increased, thus putting further constraints on cosmological timescales (Demarque, Deliyannis, & Sarajedini 1991).

Table 1 lists some of the internal properties of the current age solar models. It shows to what degree the structure of the solar model is affected by the different varying G cosmologies. Even though there appears to be quite large variations in the central hydrogen abundance, which quantifies the rate of nuclear burning in the Sun, there is no direct way to observe these differences. Similarly the differences in core temperature and density are not directly observable, except perhaps through solar neutrino experiments.

The depth of the convective envelope changes slightly with β. The depth of the convective envelope can be determined directly from observation by inverting the solar p-mode data. This will be discussed in Section 3.2. The temperature at the base of the convection zone can be constrained to some degree by observations of the abundances of the lithium and beryllium. ^{7}Li burns at temperatures above 2.4×10^6K and ^{9}Be at temperatures above 3.2×10^6K (see e.g. Clayton 1983). If the convective envelope of the Sun, during its evolution to the present day, dips deep enough in the Sun, for example, to hit temperatures above 3.2×10^6K, then all Be and Li will be quickly burned in the Sun's convective envelope and no Be or Li will be observable at the surface. Interestingly, we observe that Li has been depleted, but not entirely, and Be has not, implying that the base of the convection zone is at a temperature not much less than 2.4×10^6K (Pinsonneault et al.1989). As the table shows, values of $\beta > 0.400$ can be ruled out simply because the convection zone is too deep and all Li is destroyed rapidly. It is not possible at this point to set a stronger constraint on β because, as is well known, standard stellar models predict very little Li depletion in the present Sun, and one has to have recourse to additional mixing below the convection zone (such as turbulence induced by rotational shear) to explain the observed Li depletion (Pinsonneault et al. 1989). The efficiency of this turbulent mixing is still very uncertain.

Another observable quantity predicted by the models which yields information about the solar interior is the neutrino flux. It has long been realized that the increased central temperatures in solar models with $\beta > 0$ will result in higher predicted ^{37}Cl neutrino fluxes (Ezer and Cameron 1966; Shaviv and Bahcall 1969). Similarly, for $\beta < 0$, the predicted neutrino flux is decreased. Because of the continued interest in solar neutrinos, we give in Table 2 the sensitivity of the predicted neutrino flux on β for each of the ^{7}Li, ^{37}Cl, ^{71}Ga, ^{81}Br, ^{98}Mo and ^{115}In detectors. All fluxes are expressed in SNU's. They were calculated by combining the relevant nuclear energy fluxes from the models with the neutrino absorption cross sections averaged over energy spectra for each detector from Table 8.2 of Bahcall (1989) with the exception of ^{37}Cl which is due to Garcia et al. (1991).

3.2 *P*-mode Frequencies

In Figure 4 we plot the differences in *p*-mode frequencies of two solar models calculated with a varying *G*, $\beta = 0.100$ and $\beta = -0.100$, and a reference non-varying *G* solar model versus the *p*-mode frequencies of the non-varying *G* solar model. The numbers label the *l* values of the iso-*l* value curves. Clearly, for $\beta = 0.100$ the low *l*-value *p*-mode frequencies of the varying *G* based models are smaller than the non-varying *G* models, and the high *l*-value *p*-mode frequencies are larger. The transition occurs for *p*-modes between $l = 20$ and $l = 80$. The opposite is true for $\beta = -0.100$.

This characteristic behavior is not unique and has been discussed in the context of other non-standard solar models. For example, Guenther et al. (1993) show that the *p*-mode frequencies of a solar model that accounts for the diffusion of helium out of the surface layers compared to a standard solar model that does not are perturbed in the same manner as shown here for the varying *G* solar models. As explained in Guenther et al. (1993), the *p*-modes are primarily responding to the different location of the base of the convection zone.

To understand this characteristic behavior more completely, consider figure 1 which shows that the lower turning radius, i.e., the depth to which a particular mode can feel, is determined by its frequency and l value. P-modes with l-values greater than 80 for frequencies between 2000 μHz and 5000 μHz are all confined to upper layers of the Sun, never extending below $R = 0.7\ R_S$ the radius of the Sun's convection zone. As one follows the p-modes to lower l values the inner turning point for the modes crosses then extends below the base of the Sun's convection zone. For modes with frequencies in the range 2000–5000 μHz the transition occurs for l-values between 20 and 80.

In Figure 5, we have taken several selected p-modes and plotted their frequency differences (varying G minus constant G_0) versus β. The amplitude of the perturbation to the frequencies is very nearly linearly proportional to the power of the power law variation. This is expected since the effect of the varying G on the structure of the solar model is small; hence the effect of the structural variations on the frequencies is predominately first order.

The frequency perturbation for some modes is positive and for others it is negative. For $\beta = 0.008$ (indicated by the vertical dashed line in figure 5), which corresponds approximately to the upper limit set by cosmological nucleosynthesis in the early universe, the perturbation to the frequencies is less than 0.2 μHz. We note that the p-mode frequencies are observed to an accuracy of approximately ±0.1 μHz.

One of the successes of helioseismology has been the accurate determination of the position of the base of the convection zone (at 0.713 ± 0.003 of the solar radius) by inversion of the observed solar p-modes (Christensen-Dalsgaard et al. 1991). At the base of the convection zone, the temperature gradient in the model changes, becoming nearly adiabatic in the convective envelope. With respect to making comparisons of the frequency spectra of different solar models, the different positions of this change in temperature gradient, i.e., the location of the base of the convection zone, is the most distinguishing structural difference among the models (see Table 1). But unfortunately,

the position of the base of the convection zone in solar models is known to be sensitive to the mixing length parameter, the helium abundance, the opacities, the equation of state, the age of the model, and the surface boundary conditions. In addition, its position is known to be sensitive to the degree of helium diffusion taking place, and is probably sensitive to unexplored physics such as the strength of the magnetic fields in this region.

The primary effect of varying G cosmologies on the solar model structure is to perturb the position of the base of the convection zone. In fact, it is the different α and Y required by the varying G models that is ultimately producing a change in the position of the convection base. Unfortunately there are other ways to produce identical perturbations to the structure; hence it is not possible at this time to distinguish the different causes.

In order to determine the observability of the varying G based models we must compare the perturbations in the frequencies due to varying G to perturbations in the frequencies due to other uncertainties in the model. In Figures 6a and 6b we plot the frequency differences between the varying G models and the Sun's observed frequencies (Libbrecht, Woodard & Kaufman 1990) versus the observed frequencies. One sigma errors associated with the observations are approximately ± 0.1 μHz. In this figure, a perfect match between theory and observation would appear as a loci of points scattered horizontally along a line that intercepts the y-axis at zero. The $\beta = 0.000$ panel shows how well the predicted p-mode frequencies of current standard solar models match the observations.

Two sources of error have been identified in the solar model that are believed to be the cause of the discrepancy between theory and observation. The thickness of the bundle of lines (in figure 6, $\beta = 0.0$) is associated with errors in the interior structure and is believed to be, for the most part, due to uncertainties in the opacities and the equation of state, which can, for example, introduce errors of the order of ± 5 μHz. The non-horizontal slope of the curves in Figures 6a and 6b are associated with errors in the surface boundary conditions. More detailed and thorough discussions of the sources of

error in the solar model as revealed by the p-mode oscillation spectrum can be found in Cox et al. (1989), Guzik and Cox (1991, 1993), Guenther et al. (1992a) and Bahcall and Pinsonneault (1992).

It is clear from figures 6a and 6b that the errors in physics and constraints of the solar model introduce uncertainties in the p-mode frequencies from 0 to 10 μHz, relative to the observed frequencies. Therefore, only varying G cosmologies with $\beta > 0.4$ and $\beta < -0.4$ can be ruled out. We note that the spread in the bundle of lines increases for $\beta > 0.10$ and $\beta < -0.05$ implying that the corresponding solar models do not "look" as good. Unfortunately, we are not justified in concluding that the varying G cosmology is wrong since other errors of the model physics could compensate for some of this spread.

Because much of the error in the physics is associated with the outer layers, it is expected that current and future observations involving networks of telescopes around the world, such as the GONG and IRIS networks, will significantly reduce the observational error associated with the high l-valued modes and permit a fine tuning of the outer layers in the solar model. This in turn should reduce the non-zero slope error and make it possible to improve the varying G cosmological constraint by up to a factor of 5, allowing one to rule out varying G cosmologies with $|\beta| > 0.1$.

Although helioseismology cannot currently provide more stringent constraints on the variation of G over the past 4.5 Gyr we note that the quality of the solar models and helioseismic observations are expected to improve over the next ten years, and hence, the constraint will be refined. Moreover, combining this result with other solar observables does allow one to tighten the constraints. Given the lack of other such direct tests of the variation of G over cosmic, but recent, timescales, the present results are encouraging.

4. SUMMARY AND CONCLUSIONS

The main merit of helioseismology in testing G-variability is that it is sufficiently sensitive to test the constancy of G over the integrated lifetime of the Sun (4.5 Gyr, nearly half the age of the Galactic disk) extending into the present era. At this point, the solar p-mode frequency spectrum, coupled with state-of-the-art solar models, can be used to set a firm limit of $\beta < 0.4$ and $\beta > -0.4$ for monotonic G variability. For non-monotonic variability, this result suggests that long timescale deviations of greater than about 15% in G are ruled out. At the same time the increased scatter in the $(\nu_\beta - \nu_s)$ (see Fig. 6a and 6b) helioseismic data suggest that $\beta < 0.1$ and $\beta > -0.1$ might also be ruled out, bearing in mind that other effects may be responsible for this scatter within the uncertainties in model physics. This conclusion is in line with other astronomical evidence, leading to the constraint that G cannot have varied by more than about 5% over the solar history. With the completion of the GONG global network and the launch of the SOHO space mission in the near future, we can expect a reduction of a factor of five in the measured uncertainties of the p-mode frequencies, which will allow us to test G variability down to lower values of β. Thus the current firmest conclusion from p-modes tests G variability at the same level of precision as planetary motions and pulsar timing measurements, with the prospect of an improvement by at least a factor of five in the near future in the sensitivity of helioseismic observations. Moreover, because of the sensitivity of this test to the integrated solar history, it may help to rule out models in which variations in G have died down over cosmological time.

We have also found that the position of the base of the solar convection zone depends sensitively on variations in G. This parameter can be derived by inversion of the p-mode data. Unfortunately, it is also sensitive at the same level to model uncertainties such as the radiative opacities, the efficiency of helium diffusion, turbulence induced by rotational shear and the likely presence of magnetic fields. Only when the relative

importance of these effects are better understood will it become possible to test the possibility of a varying G in this way.

Finally, there are the g-modes. There is still no consensus as to whether g-modes have been observed on the Sun, or even whether they can be observed at all at the solar surface, because g-mode amplitudes are known to be attenuated in the convection zone. Claims of g-mode observations are still controversial (Henning and Scherrer 1988; Hill and Gu 1990). However, because g-modes probe the central regions of the Sun more completely than p-modes, the g-mode spectrum is more sensitive to variations in G and can provide and order of magnitude stronger constraint than p-modes. This will be discussed in (Guenther, et al. 1994). Space missions such as the planned SOHO GOLF (Damé 1988) and SDS (Sofia et al. 1991) experiments offer at this time the best prospects for detecting solar g-modes and measuring their periods reliably.

This research is supported in part by NASA grants NAGW-2531 and NAG5-1486 to Yale University, and by funds from Case Western Reserve University.

REFERENCES

Accetta, F.S., Krauss, L.M. & Romanelli P. 1990, Phys. Lett. B248, 146

Bahcall, J. N. 1989, Neutrino Astrophysics (Cambridge U.P.: Cambridge)

Bahcall, J. N. and Pinsonneault, M. H. 1992, Rev. Mod. Phys.

Brans, C. and Dicke, R. H. 1961, Phys. Rev., 124, 925

Christensen-Dalsgaard, J., Gough, D.O., & Thompson, M.J. 1991, ApJ, 378, 413

Clayton, D.D. 1983, Principles of Stellar Evolution and Nucleosynthesis, 2nd ed., (U. of Chicago P.: Chicago)

Cohen, E. R., & Taylor, B. N. 1986, Codata Bulletin No. 63, (New York: Pergamon Press)

Cox, A. N., Guzik, J. A., & Kidman, R. B. 1989, ApJ, 342, 118

Damé, L. 1988, Proc. Symp. "Sun and Sun-like Stars", ed. E.J. Rolfe, ESA SP-286, p.367

Damour , T., Gibbons, G.W., and Taylor, J..H. 1988, Phys. Rev. Lett., 61, 1151

Demarque, P. and Guenther, D. B. 1991, in "Solar Interior and Atmosphere," ed. A. Cox, W. Livingston, and S. Mathews, Chapter 33, (U. of Arizona P.: Tucson)

Demarque, P., Deliyannis, C. P., & Sarajedini, A. 1991, in "Observational Tests of Cosmological Inflation," eds. T. Shanks et al., Kluwer Academic Pub., p.111

Dicke, R. H. and Peebles, P. J. E. 1965, Space Sci. Rev., 4, 419

Dirac, P. A. M. 1938, Proc. R. Soc., A165, 199

Ezer, D. and Cameron, A.*G*.W. 1966, Can. J. Phys., 44, 593

Gamow, G. 1967, Proc.N.A.S., 57, 187

Garcia, et al. 1991, Phys. Rev. L. 67, 3654

Guenther, D. B. 1989, ApJ, 339, 1156

Guenther, D. B. 1994, ApJ, 442, 000

Guenther, D. B., Demarque, P., Kim, Y. -C., and Pinsonneault, M. H. 1992a, ApJ, 387, 371

Guenther, D. B., Pinsonneault, M. H., and Bahcall, J. N. 1993, ApJ, 418, 000

Guenther, D.B., Demarque, P., Pinsonneault, M.H. and Kim, Y.-C. 1992b, ApJ, 392, 328

Guenther, D. B., Sills, K., & Demarque, P., Lawrence Krauss 1994, ApJ, in preparation

Guzik, J. A. & Cox, A. N. 1991, ApJ, 381, 333

Guzik, J. A. & Cox, A. N. 1993, ApJ, 411, 394

Henning, H.M. and Scherrer, P.H. 1988, Proc. Symp. Sun and Sun-Like Stars, ed. E.J. Rolfe, ESA SP-286, p.419

Hill, H.A. and Gu, Ye-ming 1990, Science in China (Series A) 37, No.7, 854

Krauss , L.M. and White, M. 1992, Ap. J. 394, 385

La, P., and Steinhardt, P.J. 1989, Phys. Rev. Lett., 62, 376

Libbrecht, K. G., Woodard, M. F., & Kaufman, J. M. 1990, ApJS, 74, 1129

Marciano, W.J. 1984, Phys. Rev. Lett. 52, 489

Pinsonneault, M.H., Kawaler, S.D., Sofia, S. and Demarque, P. 1989, ApJ, 338, 424

Pochoda, P. and Schwarzschild, M. 1964, ApJ, 139, 587

Prather, M.J. 1976, Ph.D. thesis, Yale University

Reasenberg, R. D. 1983, Phil. Trans. Roy. Soc., London, A310, 227

Roeder, R.C. 1967, ApJ, 149, 131

Roeder, R.C. and Demarque, P. 1966, ApJ, 144, 1016

Saio, H. and Cox, J. P. 1980, ApJ, 236, 549

Schwarzschild, M. 1958, Structure and Evolution of the Stars (Princeton U.P.: Princeton)

Shapiro , I.I. 1964, Phys. Rev. Lett., 13, 789

Shapiro, I.I. et al. 1971, Phys. Rev. Lett., 26, 1132

Shaviv, G. and Bahcall, J.N. 1969, Ap.J.155,135

Sofia, S., Maier, E. and Twigg, L. 1991 Adv. Space Res., 11, 123

Steinhardt, P.J. & Accetta, F.S. 1990, Phys. Rev. Lett., 62, 2740

Teller, E. 1948, Phys.Rev., 73, 801

Tinsley, B. M. 1972, ApJL, 174, L119

Unno, W., Osaki, Y., Ando, H., & Shibahashi, H. 1989, "Nonradial Oscillations of Stars," Second Edition (Tokyo: University of Tokyo Press)

Wesson, P. S. 1973, Quart. J. R. A. S., 14, 9

TABLE 1

MODEL CHARACTERISTICS

β	α	X	X_{core}	log T_{core}	log ρ_{core}	R_{env}/R_s	T_{env}
–0.400	1.832	0.6942	0.456	7.1800	2.0986	0.739	1.988E6
–0.200	1.895	0.7010	0.421	7.1841	2.1270	0.731	2.062E6
–0.100	1.936	0.7051	0.400	7.1866	2.1445	0.724	2.108E6
–0.050	1.959	0.7074	0.388	7.1879	2.1544	0.723	2.126E6
–0.025	1.971	0.7085	0.382	7.1887	2.1596	0.723	2.132E6
0.000	1.983	0.7098	0.376	7.1894	2.1650	0.721	2.148E6
0.025	1.996	0.7110	0.369	7.1902	2.1707	0.720	2.150E6
0.050	2.009	0.7123	0.362	7.1910	2.1766	0.719	2.171E6
0.100	2.036	0.7151	0.348	7.1927	2.1891	0.716	2.193E6
0.200	2.104	0.7405	0.317	7.1965	2.2177	0.710	2.255E6
0.400	2.291	0.7356	0.239	7.2059	2.2951	0.695	2.392E6

TABLE 2

SOLAR NEUTRINO FLUXES OF MODELS

β	^{7}Li	^{37}Cl	^{71}Ga	^{81}Br	^{98}Mo	^{115}In
0.2	51.8	8.68	134.	29.6	18.8	641.
0.0	42.0	6.75	124.	23.6	14.3	619.
–0.2	35.9	5.5	117.	19.7	11.3	604.

FIGURE CAPTIONS

Figure 1. Five curves representing p-mode frequencies at 1000 μHz, 2000 μHz,... 5000 μHz show the radius of the inner turning point of a p-mode versus $(l(l+1))^{1/2} \approx l$. For example, the inner turning point of an $l = 100$ p-mode with a frequency of 3000 μHz is at radius $0.9R_s$. Below this radius the mode is exponentially damped.

Figure 2. For $G(t) \propto t^{-\beta}$, the normalized value of G is plotted opposite age of the universe for several different values of β. The present day age of the Universe is taken to be 15 Gyr.

Figure 3. Evolutionary tracks of the solar model from zero age to present day under the assumption of a power law variation in G are drawn in the HR-diagram. The $\beta = 0.0$ track (dashed line) corresponds to a constant G.

Figure 4. The frequency differences, varying G based models ($\beta = \pm 0.100$) minus constant G_0 based models ($\beta = 0.000$), are plotted opposite the frequencies of the constant G_0 based models. Numbers identify lines connecting p-modes of similar degree.

Figure 5. The frequency differences, varying G based models ($\beta \neq 0.000$) minus constant G_0 based models ($\beta = 0.000$), of several selected p-modes are plotted opposite β the exponent of the power law variation in G. The vertical dashed line drawn in (b) corresponds to the largest value of β tolerated in the early universe according to constraints set by cosmological nucleosynthesis. The ($\beta = 0.0$) frequencies are 3761.38, 3072.89, 4142.67, and 4064.95 μHz for the chosen l=3,20,60,300 modes respectively.

Figure 6. The frequency differences, model (ν_β) minus Sun (ν_s), are plotted opposite the observed frequencies of the modes (Libbrecht, Woodard, & Kaufman 1990). Only selected modes (see Fig. 4) with l-values less 150 are plotted.

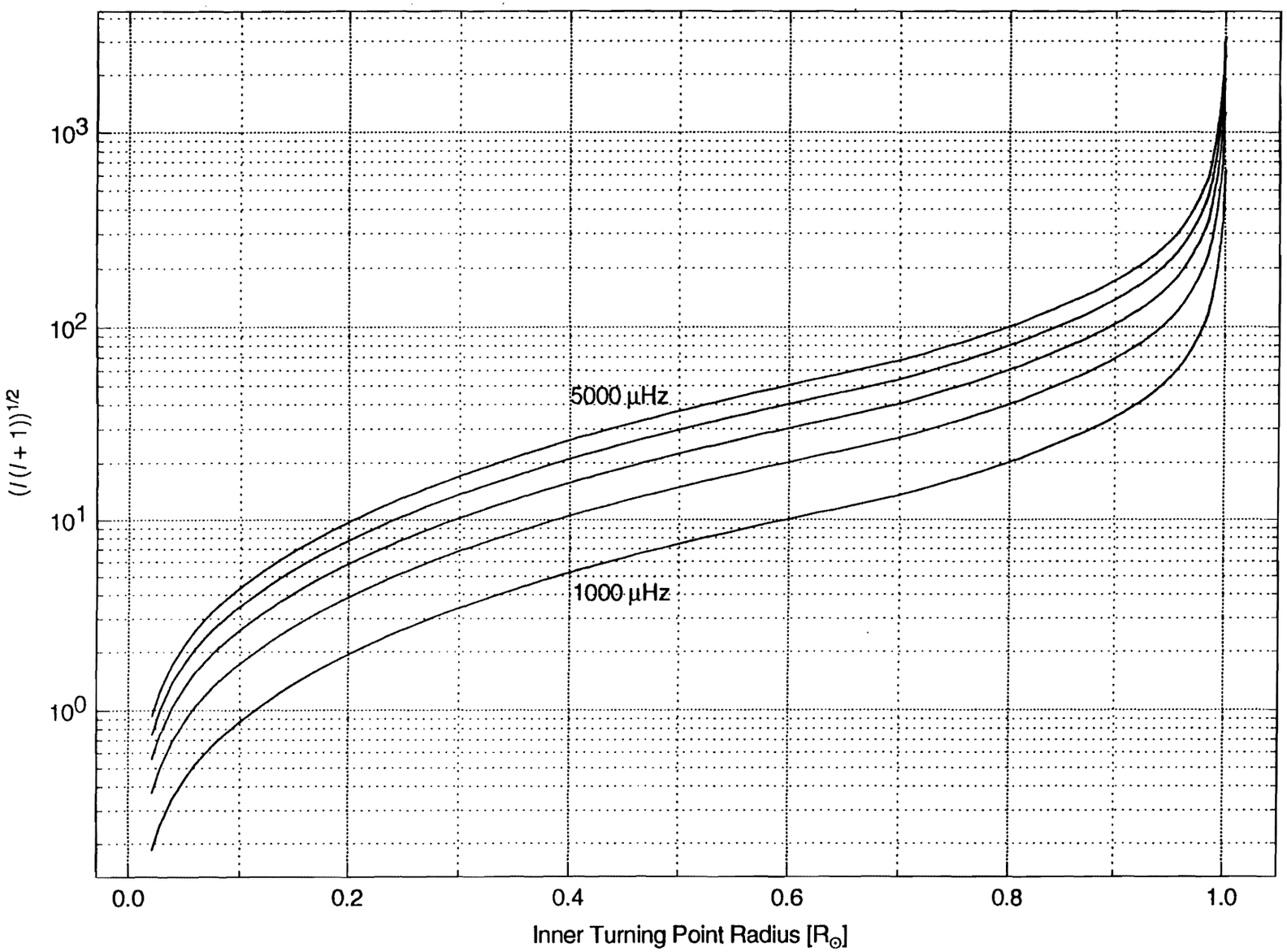
10^3
10^2
10^1
10^0
$(l(l+1))^{1/2}$
5000 μHz
1000 μHz
0.0
0.2
0.4
0.6
0.8
1.0
Inner Turning Point Radius [$R_\odot$]

Figure 1

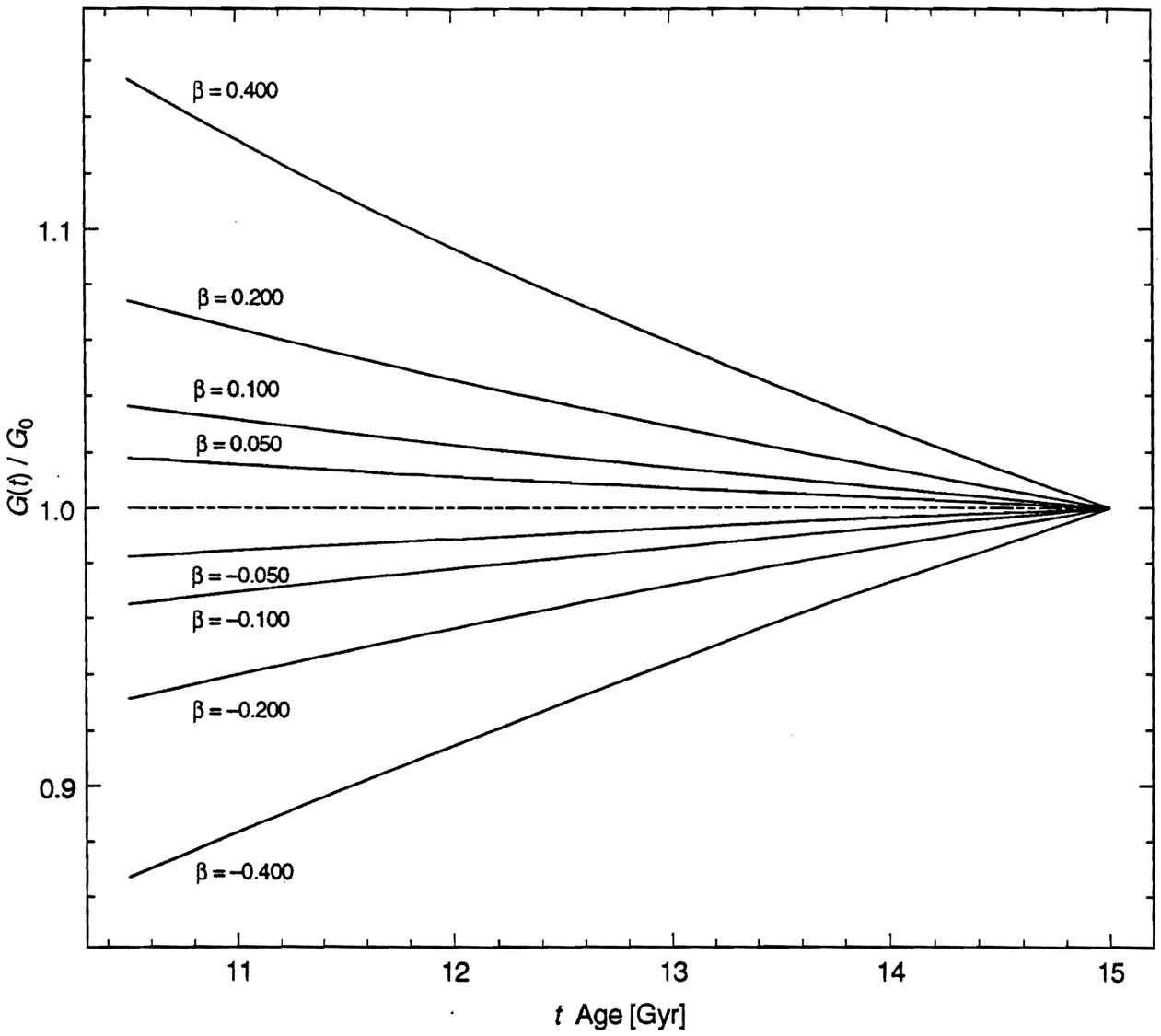
β = 0.400
β = 0.200
β = 0.100
β = 0.050
β = −0.050
β = −0.100
β = −0.200
β = −0.400
1.1
1.0
0.9
G(t) / G0
11
12
13
14
15
t Age [Gyr]

Figure 2

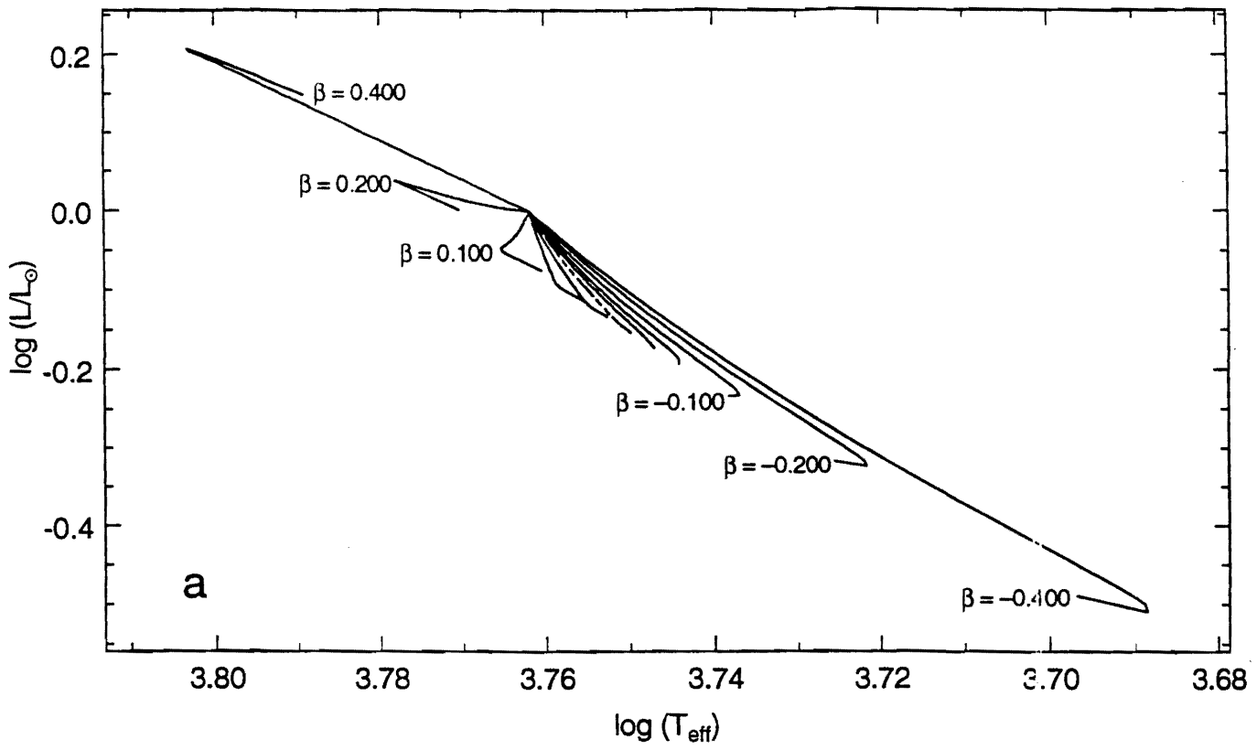
0.2
0.0
-0.2
-0.4
log (L/L⊙)
β = 0.400
β = 0.200
β = 0.100
β = −0.100
β = −0.200
β = −0.400
a
3.80
3.78
3.76
3.74
3.72
3.70
3.68
log (Teff)

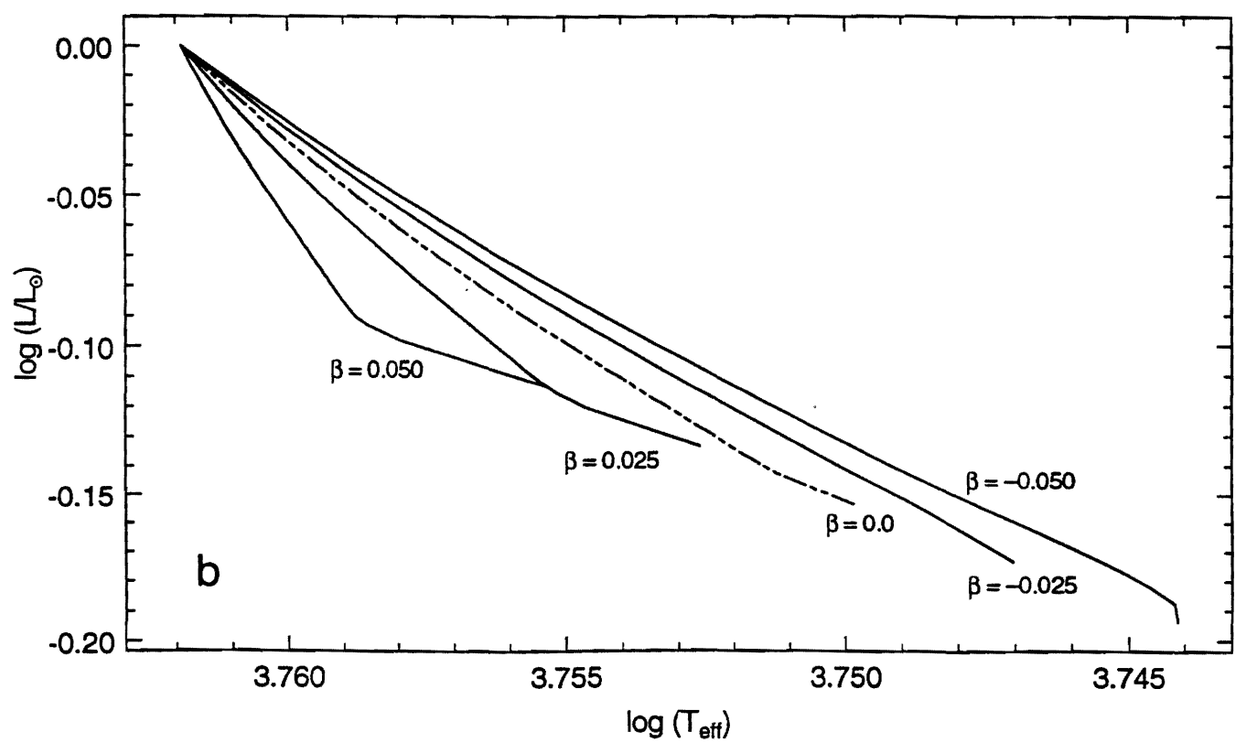
0.00
-0.05
-0.10
-0.15
-0.20
log (L/L⊙)
β = 0.050
β = 0.025
β = 0.0
β = −0.050
β = −0.025
b
3.760
3.755
3.750
3.745
log (Teff)

Figure 3a & b

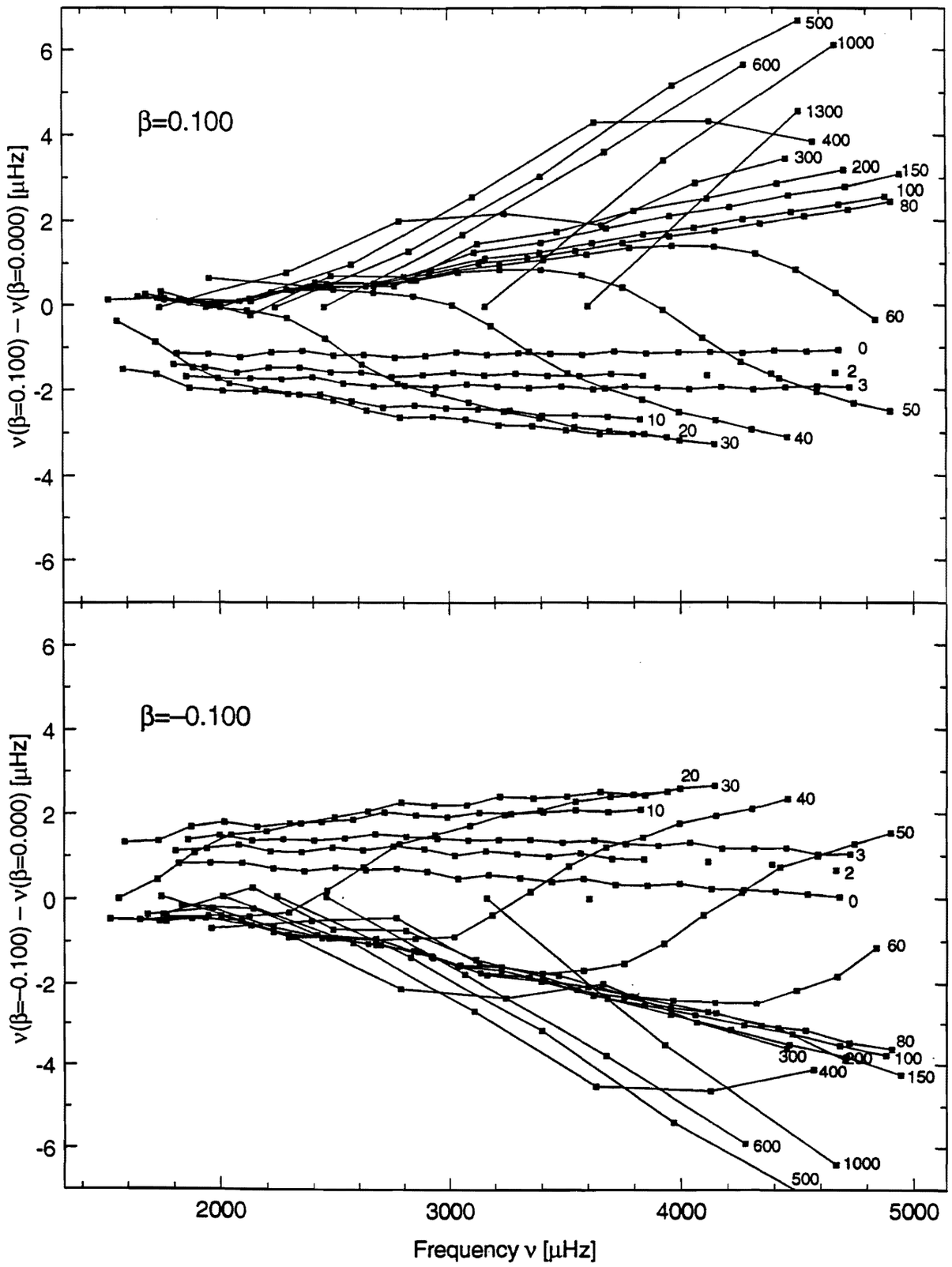
β=0.100
β=−0.100
ν(β=0.100) − ν(β=0.000) [μHz]
ν(β=−0.100) − ν(β=0.000) [μHz]
Frequency ν [μHz]
2000
3000
4000
5000
6
4
2
0
-2
-4
-6
500
1000
600
1300
400
300
200
150
100
80
60
0
2
3
50
10
20
30
40

Figure 4

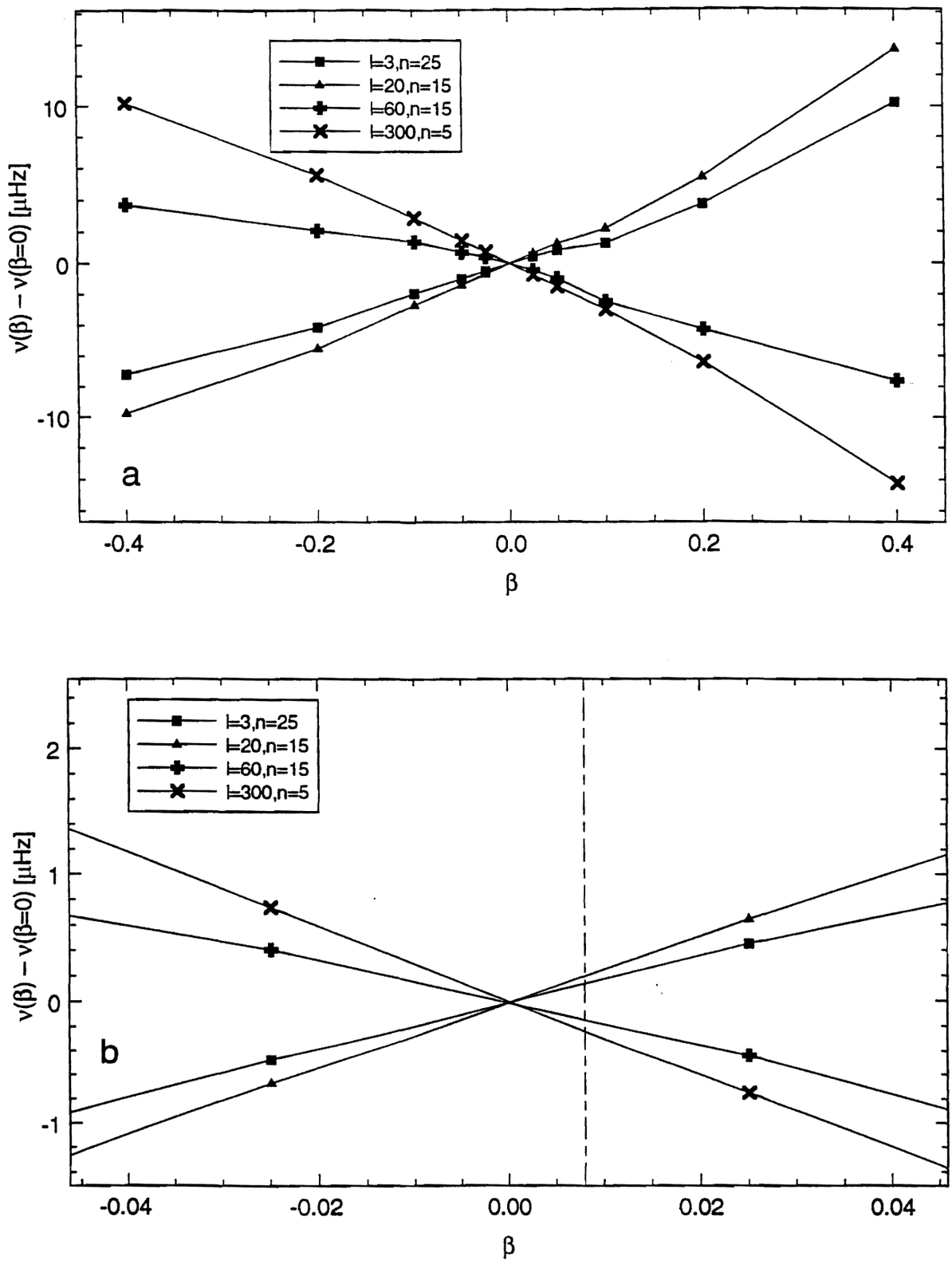

Figure 5

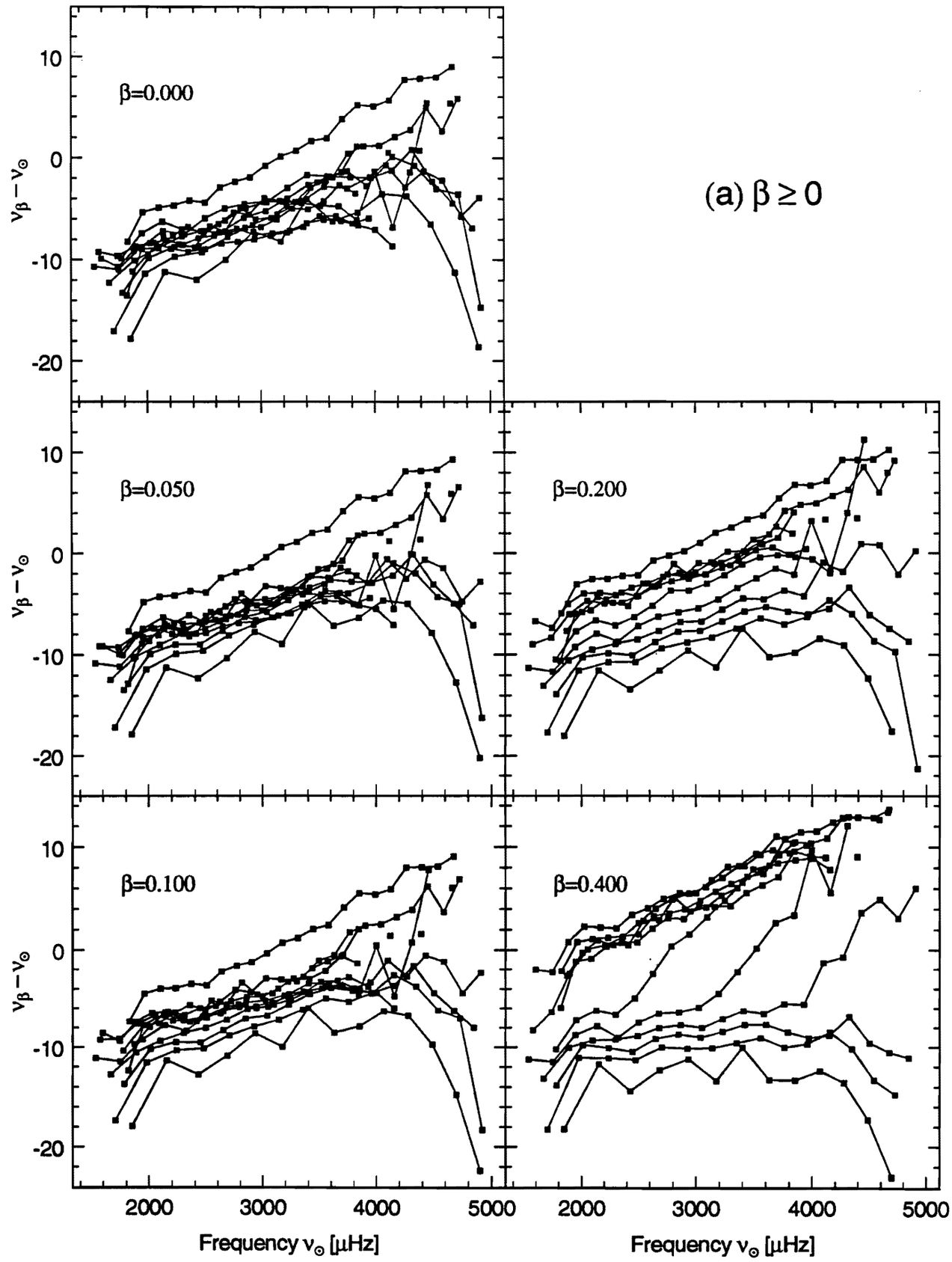
(a) β ≥ 0
β=0.000
β=0.050
β=0.100
β=0.200
β=0.400
$\nu_\beta - \nu_\odot$
10
0
-10
-20
2000
3000
4000
5000
Frequency $\nu_\odot$ [μHz]

Figure 6a

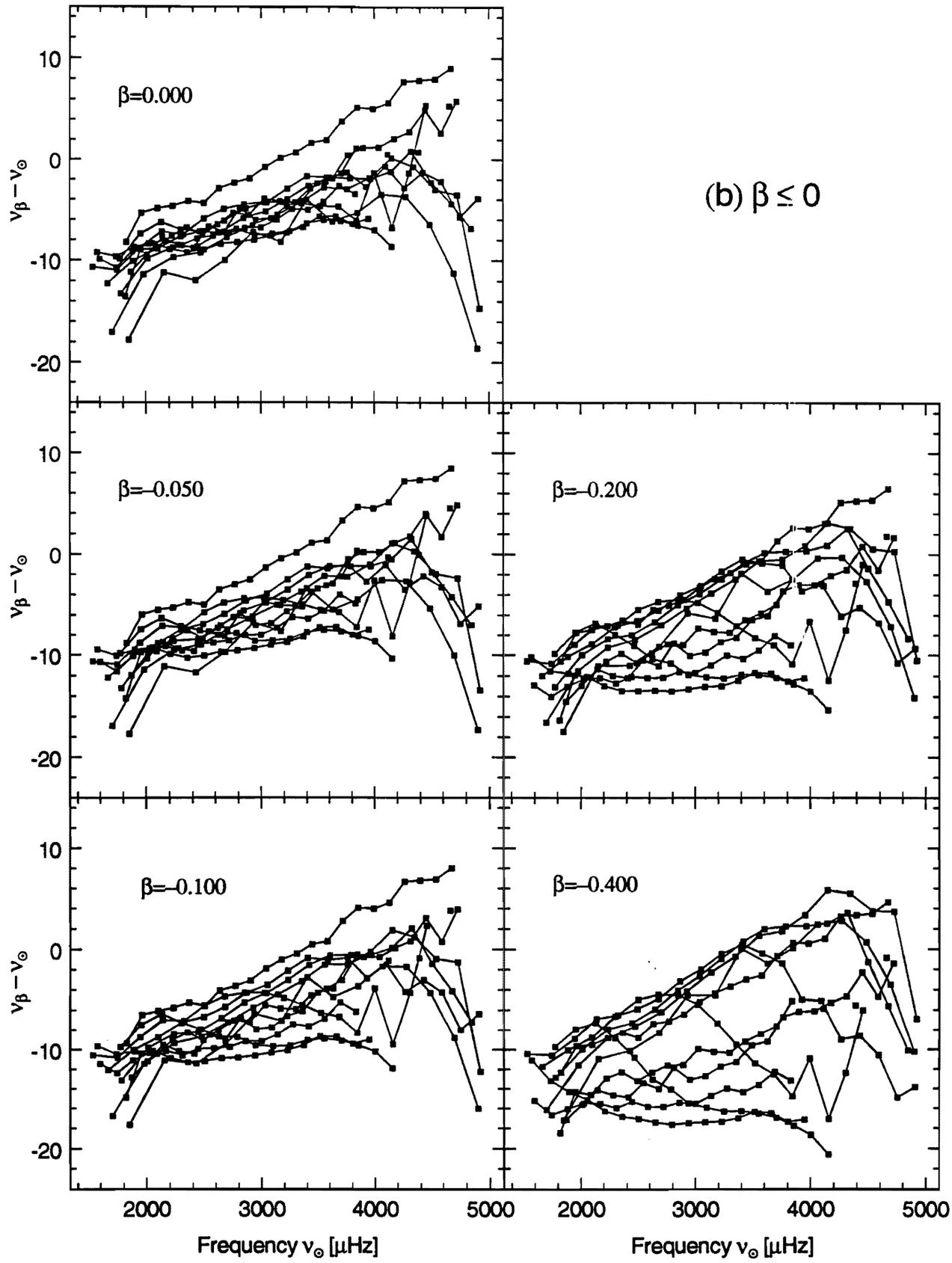
(b) β ≤ 0
β=0.000
β=–0.050
β=–0.200
β=–0.100
β=–0.400
$\nu_\beta - \nu_\odot$
10
0
-10
-20
2000
3000
4000
5000
Frequency $\nu_\odot$ [μHz]

Figure 6b